Receptor for activated C kinase 1 promotes cervical cancer lymph node metastasis via the glycolysis-dependent AKT/mTOR signaling

LIXIU XU[1*], JINQIU LI[1*], MIKRBAN TURSUN[1], YAN HAI[1], HATILA TURSUN[1], BATUR MAMTIMIN[2] and AYSHAMGUL HASIM[1]

[1]Department of Basic Medicine, Xinjiang Medical University and Xinjiang Key Laboratory of Molecular Biology of Endemic Diseases; [2]Department of Pharmacy, Xinjiang Medical University, Urumqi, Xinjiang 830017, P.R. China

Received February 3, 2022; Accepted May 6, 2022

DOI: 10.3892/ijo.2022.5373

Abstract. Cervical cancer (CC), an aggressive form of squamous cell carcinoma, is characterized by early-stage lymph node metastasis and an extremely poor prognosis. The authors have previously demonstrated that patients with CC have aberrant glycolysis. The upregulation of receptor for activated C kinase 1 (RACK1) is associated with CC lymph node metastasis (LNM). However, its role in mediating aerobic glycolysis in CC LNM remains unclear. In the present study, ^{1}H nuclear magnetic resonance analysis revealed a significant association between RACK1 expression and the glycolysis/gluconeogenesis pathway. Additionally, *RACK1* knockdown inhibited aerobic glycolysis and lymphangiogenesis *in vitro* and suppressed CC LNM *in vivo*. Furthermore, protein kinase B (AKT)/mammalian target of rapamycin (mTOR) signaling was identified as a critical RACK1-regulated pathway that increased lymphangiogenesis in CC. Co-immunoprecipitation, immunofluorescence and western blot analysis revealed that RACK1 activated AKT/mTOR signaling by interacting with insulin-like growth factor 1 receptor (IGF1R). POU class 2 homeobox 2 (POU2F2) bound to the *RACK1* promoter and regulated its transcription, thereby functionally contributing to glycolysis and lymphangiogenesis in CC. Of note, the administration of 2-deoxy-D-glucose, which attenuates glycolysis, inhibited RACK1-induced lymphangiogenesis in CC. The correlations between RACK1, IGF1R, POU2F2 and hexokinase 2 were further confirmed in CC tissues. Thus, RACK1 plays a crucial role in CC tumor LNM by regulating glycolysis via IGF1R/AKT/mTOR signaling. Thus, the targeting of the POU2F2/RACK1/IGF1R/AKT/mTOR signaling pathway may provide a novel treatment strategy for CC.

Correspondence to: Professor Ayshamgul Hasim, Department of Basic Medicine, Xinjiang Medical University and Xinjiang Key Laboratory of Molecular Biology of Endemic Diseases, 567 Shangde North Road, Urumqi, Xinjiang 830017, P.R. China
E-mail: axiangu75@126.com

*Contributed equally

Abbreviations: CC, cervical cancer; RACK1, receptor for activated C kinase 1; IGF1R, insulin-like growth factor 1 receptor; POU2F2, POU class 2 homeobox 2; AKT, protein kinase B; mTOR, mammalian target of rapamycin; HK2, hexokinase 2; LDHA, lactate dehydrogenase A; GLUT1, glucose transporter 1; PKM2, pyruvate kinase M2; PDPN, podoplanin; 2-DG, 2-deoxy-D-glucose; LNM, lymph node metastasis; IHC, immunohistochemistry; ^{1}H NMR, ^{1}H nuclear magnetic resonance; shRNA, short hairpin RNA; Co-IP, co-immunoprecipitation; Rapa, rapamycin; ChIP, chromatin immunoprecipitation

Key words: cervical cancer, RACK1, AKT/mTOR signaling, glycolysis, lymph node metastasis

Introduction

Cervical cancer (CC) is the fourth-most common malignancy affecting women worldwide, and the gradual increase in its incidence and mortality has attracted considerable attention (1). In particular, the incidence and mortality due to CC is high in the Xinjiang region of China (2). Metastasis is responsible for >90% of cancer-related deaths, and effective therapies for metastatic cancer are limited (3). Lymph node metastasis (LNM) and blood metastasis are common in the early and late stages of the disease, respectively. CC mainly metastasizes via the lymphatic vessels and direct extension (4). Therefore, the prevention of LNM is critical for CC therapy. Accumulating evidence suggests that LNM is a complex process involving mechanical forces within the tumor and host tissues, as well as molecular factors contributed by tumor cell proliferation, cytokine production and lymphangiogenesis (5). Lymphangiogenesis involves the migration of endothelial cells into tumors and formation of new lymph vessels (6,7). However, lymphangiogenesis and its regulatory mechanisms in CC remain unclear.

Metabolic changes are now considered biomarkers for distinguishing the characteristics of metastatic tumors (8). Alterations in glucose metabolism, characterized by an increased aerobic glycolysis (the Warburg effect), is well-established as one of the hallmarks of cancer (9), which contributes to tumor

growth and metastasis by providing energy and substrates for biosynthesis (10,11). The authors previously tested plasma samples from patients with CC and healthy individuals using ^{1}H-nuclear magnetic resonance (^{1}H-NMR)-based untargeted metabolomics and found that glycolysis-related enzymes were upregulated in CC tissues (12). This highlights the importance of aerobic glycolysis in the progression of CC.

Receptor for activated C kinase 1 (RACK1) receptor, a multifunctional scaffolding protein, is involved in nucleating cell signaling hubs, regulating protein activity, and modulating the migration and invasion of tumor cells (13). A previous study demonstrated that RACK1 was highly expressed in CC tissues and positively associated with the poor prognosis of patients with CC (14). However, the metabolic significance and biological function of RACK1 in CC remain unclear. Based on the aforementioned evidence, it was hypothesized that RACK1 promotes LNM by regulating glycolysis in CC.

The present study investigated whether RACK1 facilitates CC progression. RACK1 was found to regulate glycolysis and lymphangiogenesis by interacting with insulin-like growth factor 1 receptor (IGF1R) and activating protein kinase B (AKT)/mammalian target of rapamycin (mTOR) signaling. In addition, the POU class 2 homeobox 2 (POU2F2)-mediated overexpression of RACK1 modulated the malignant progression of CC via the sustained activation of the AKT/mTOR signaling pathway. The findings presented herein reveal potential novel mechanisms for CC LMN and provide promising novel therapeutic targets. These novel therapeutic targets and treatment options may effectively prevent the aggressiveness of CC.

Materials and methods

Clinical samples. CC tissues (n=104; age range, 28-68 years; mean age, 49.52±8.90 years) and normal adjacent cervical epithelial tissues [used as a negative control (NC), n=31; age range, 21-56 years; mean age, 40.81±9.45 years] were collected from the Department of Pathology of First Affiliated Hospital of Xinjiang Medical University (Urumqi, China) between April, 2011 and June, 2021. The normal adjacent cervical epithelial tissues were collected >3 cm from the tumor edge. The inclusion criteria for patient recruitment were as follows: i) None of the patients received chemotherapy or radiation prior to surgery; ii) a confirmed the diagnosis by two pathologists; and iii) patients who agreed to participate in the study. The exclusion criteria were as follows: i) Patients with other diseases, including other types of tumors; and ii) patients who refused to participate in the study. The patients with CC were diagnosed by histopathological analysis according to the tumor-node-metastasis (TNM) classification of the International Federation of Gynecology and Obstetrics (FIGO) (15). The study was carried out in accordance with the guidelines of the Ethics Committee of the First Affiliated Hospital of Xinjiang Medical University (authorization no. IACUC-20180223-128). Written informed consent was obtained from all patients and their relatives.

Cells and cell culture. Human CC cell lines [MS751 (cat. no. CL-0387), SiHa (cat. no. CL-0210), HeLa (cat. no. CL-0101) and Caski (cat. no. CL-0048)], H8 (cat. no. CP-H059), an immortalized cervical epithelial cell line, and human lymphatic endothelial cells (HLECs, cat. no. CP-H026) were purchased from Procell Life Science & Technology Co., Ltd. The SiHa, HeLa and H8 cells were cultured in Dulbecco's modified Eagle's medium (DMEM) supplemented with penicillin/streptomycin and fetal bovine serum (FBS) (Gibco; Thermo Fisher Scientific, Inc.). The MS751 cells were cultured in minimal essential medium (MEM; containing NEAA) medium (Procell Life Science & Technology Co., Ltd.) supplemented with 10% FBS, and the Caski cells were cultured in Roswell park Memorial Institute (RPMI)-1640 medium (Biological Industries) supplemented with penicillin/streptomycin (Biological Industries)and 10% FBS. All cell lines were authenticated using STR profiling to confirm their identities and cultured in an incubator with 5% CO_2 at 37˚C. HLECs were obtained from Procell Life Science & Technology Co., Ltd. and cultured in endothelial cell medium (ECM; ScienCell Research Laboratories, Inc.).

Lentiviral or plasmid transfection. To knockdown *RACK1*, a lentivirus containing short hairpin RNA (shRNA) targeting *RACK1* or a non-target oligonucleotide was synthesized by Shanghai Genechem Co., Ltd. The shRNA target sequences were as follows: shRACK1-1, 5'-AGCTGAAGACCAACCACAT-3'; shRACK1-2, 5'-TGTGGTTATCTCCTCAGAT-3'; non-specific control shRNA (shNON), 5'-TTCTCCGAACGTGTCACGT-3'. In brief, the lentiviral constructs for RACK1 knockdown (shRACK1) and scramble control (shNON) were constructed into GV493 (Shanghai Genechem Co., Ltd.). All the plasmids were co-transfected with pHelper 1.0 (20 μg) and pHelper 2.0 (10 μg) into 293T cells (National Collection of Authenticated Cell Cultures, Shanghai, China, https://www.cellbank.org.cn/) using transfection reagent prepared by Shanghai Genechem Co., Ltd. in accordance with the manufacturer's recommendations. The supernatant was collected after culturing for 48 h. For CC cell infection, cells ($1x10^4$ cell/well) were cultured for 24 h, and recombinant lentivirus in serum-free growth medium was then added at a multiplicity of infection (MOI=30) at 37˚C for 72 h. Stable cell lines were selected using 5 μg/ml puromycin (MilliporeSigma) and the knockdown efficiency was confirmed using western blot analysis. The POU2F2 overexpression plasmid and control plasmid were purchased from Shanghai Genechem Co., Ltd. For transient transfection, CC cells ($1x10^5$ cell/well) in 6-well plates were transfected with POU2F2 overexpression plasmid (5 μg/ml) and control plasmid (4 μg/ml) at 37˚C. After culturing for 24 h, the cells were harvested for subsequent experiments, and the overexpression efficiency was confirmed using western blot analysis. Plasmid transfections were performed using Lipofectamine® 3000 reagent (Invitrogen; Thermo Fisher Scientific, Inc.) according to the manufacturer's protocol. The overexpression target sequences are listed in Table SI.

RNA extraction and reverse transcription-quantitative polymerase chain reaction (RT-qPCR). RNA was extracted from the CC cells using Trizol® reagent (Invitrogen; Thermo Fisher Scientific, Inc.). The reverse transcription of the extracted RNA was performed using a RevertAid First Strand cDNA synthesis kit (cat. no. K1622, Thermo Fisher Scientific,

Inc.) following the manufacturer's instructions. PCR amplification was performed using the QuantiNova SYBR-Green PCR kit (cat. no. 208054, Qiagen GmbH). The cycling conditions were as follows: 95˚C for 5 sec; followed by 40 cycles at 60˚C for 10 sec, and 95˚C for 2 min. The relative expression of target genes was calculated using the $2^{-\Delta\Delta Cq}$ method (16), and *ACTB* was used as the reference gene for normalization. The sequences of the primers used are listed in Table SII.

Western blot analysis. Cells were lysed in radioimmunoprecipitation assay buffer containing a protease/phosphatase inhibitor cocktail (Beijing Solarbio Science & Technology Co., Ltd.). The protein concentration estimated using the BCA method, and total proteins (30 μg) were separated in 10% sodium dodecyl sulfate-polyacrylamide gels and transferred onto polyvinylidene fluoride membranes (MilliporeSigma). The membranes were then blocked with 5% skim milk for 2 h at room temperature and probed with primary antibodies overnight at 4˚C and horseradish-peroxidase-labeled secondary antibodies for 2 h at room temperature. Following three washes the membranes using Tris-buffered saline with Tween-20 (TBST) buffer, the signal was detected using an enhanced chemiluminescence detection system (ECL; Biosharp) and analyzed using the FluorChem™ E system (FluorChem F, ProteinSimple). The band intensities were quantified using ImageJ software (version 1.52a; National Institutes of Health). The primary and secondary antibodies used in the present study are listed in Table SIII.

Immunohistochemistry (IHC). IHC was performed on formalin-fixed paraffin-embedded sections of clinical CC and mouse xenograft tissues. The paraffin-embedded tissue sections (4-μM-thick) were rehydrated, blocked with 3% hydrogen peroxide, and treated with hot EDTA buffer (75˚C for 10 min; 50˚C for 10 min). Subsequently, primary antibodies were added and incubated overnight at 4˚C. Secondary antibody incubation (cat. no. PV9000; ZSJQ-Bio) was performed at room temperature for 30 min. Color reaction was developed using 3,3'-diaminobenzidine tetrachloride (DAB) chromogen solution. The staining intensity was scored independently by two observers. Briefly, the standard for the proportion of positive staining (1, <5%; 2, 5-30%; 3, 30-70%; 4, >70%) and staining intensity (0, no staining; 1, weak; 2, moderate; 3, strong) were multiplied for each observer and then averaged. The primary antibodies used and their corresponding experimental conditions are listed in Table SIII.

^{1}H NMR spectroscopy. ^{1}H NMR spectroscopy was used for metabolomics analysis as previously described (12). Briefly, cell supernatants were defrosted at room temperature. Each sample (200 μl) was mixed with 400 μl saline (0.9% w/v NaCl in 20% v/v D_2O and 80% v/v H_2O) at room temperature and vortex-mixed, followed by centrifugation (4˚C, 10,000 x g, 10 min). Subsequently, 550 μl supernatant were transferred into a 5-mm NMR tube for ^{1}H NMR (Varian 600 spectrometer with 599.93 MHz resonance frequency of ^{1}H NMR). Transverse relaxation weighting experiments were performed per the Carr-Purcell-Meiboom-Gill sequence with water peak suppression. Parameters were set as follows: Relaxation delay, 2.0 sec; acquisition time, 1.64 sec; and spectral width, 10,000 Hz, which resulted in an acquisition time of 1.64 sec and a relaxation delay of 2 sec. The raw data were processed according to a previous study (12). Briefly, the ^{1}H NMR spectra were processed and corrected for phase and baseline using the Topspin 2.0 software (Brokers Biospin). The baseline-corrected ^{1}H NMR spectra were manually phased, which were referenced to the anomeric proton of α-glucose at δ 5.233, and the spectra were placed into 2,834 integrated regions of 0.003 ppm. The regions of water resonance (δ 4.66-5.20) were excluded for eliminating the baseline effects. The peak area of each bin was then calculated. Normalization were performed using the SIMCA-P+11 software package (Umetrics Inc.) to compensate for the concentration differences among the samples. The spectral segments for each NMR spectrum were normalized to the total integrated area of each spectrum. Principal component analysis (PCA) and the orthogonal projection to latent structure with discriminant analysis (OPLS-DA) methods with unit variance (UV) scaling were carried out for class discrimination and biomarker identification. PCA was conducted using mean-centered scaling and the results are presented in scatter plots; each pointing the former represented one sample, whereas the latter indicated the magnitude and manners of the NMR signals (thus metabolites) to classification. The data were visualized with the score plots of the first two principal components (PCs 1 and 2) in order to provide the most efficient 2D representation of the information contained in the dataset. Based on the number of samples in each group, a correlation coefficient (determined using the Pearson's product-moment correlation coefficient) of 0.33 was used as the cut-off value that calculated discrimination at the level of P=0.05. The normalized NMR dataset was subjected to classical statistical analysis (one-way ANOVA) using SPSS 23.0 software (SPSS, Inc.).

Bioinformatics analysis. The Gene Expression Omnibus (GEO) datasets, GSE6791 dataset (https://www.ncbi.nlm.nih.gov/geo/query/acc.cgi?acc=GSE6791), GSE9750 dataset (https://www.ncbi.nlm.nih.gov/geo/query/acc.cgi?acc=GSE9750), GSE26511 dataset (https://www.ncbi.nlm.nih.gov/geo/query/acc.cgi?acc=GSE26511) were used for analyzing the expression of *RACK1* in cervical cancer tissues. Hitpredict (http://www.hitpredict.org/) and Genemania (http://genemania.org/) were used to predict the candidate factors that interacted with RACK1. The UCSC Genome Browser (http://genome-asia.ucsc.edu/index.html), HUMANTFDB (http://bioinfo.life.hust.edu.cn/HumanTFDB/#!/predict) and PROMO (http://alggen.lsi.upc.es/cgi-bin/promo_v3/promo/promoinit.cgi?dirDB=TF_8.3) were used to predict potential complementary base pairing between RACK1 and transcription factors. MetaboAnalyst (https://www.metaboanalyst.ca/) were used for analyzing the differential metabolic pathway of knockdown of RACK1 in CC cells. JASPAR database (https://jaspar.genereg.net/) were used to predict potential binding sites between RACK1 and IGF1R.

Transwell migration assay of CC cells or HLECs. For the Transwell migration assay of CC cells, 2x10^4 cells were placed in the upper chamber of a Transwell (Corning, Inc.). Basic medium containing 10% FBS was added to the lower chamber

as a chemoattractant and the cells were incubated at 37˚C for 24 h. For examining migration, HLECs ($1x10^5$) were placed in the upper chamber with serum-free EGM, whereas the lower chamber was filled with conditioned medium derived from $1x10^5$ CC cells mixed with EGM medium at a 1:1 ratio as the chemoattractant and incubated at 37˚C for 24 h. The cells that adhered to the reverse side of the membrane were fixed with 4% paraformaldehyde solution at 4˚C for 30 min and stained with 0.1% crystal violet (Beijing Solarbio Science & Technology Co., Ltd.) at room temperature for 30 min and counted under an inverted microscope (Nikon E400, Nikon Corporation) in five randomly selected fields.

Matrigel invasion assay. Matrigel-coated invasion chambers (BD Biosciences) were used to assess cell invasion. Briefly, $2x10^4$ CC cells were seeded in the upper chamber of the Transwell insert in serum-free culture medium and cultured at 37˚C for 24-48 h. The penetrated cells were fixed with 4% paraformaldehyde and stained using 0.1% crystal violet at room temperature for 30 min. The number of penetrating cells in each group was counted under an inverted microscope (Nikon E400, Nikon Corporation).

Determination of glucose consumption and lactate production. Glucose and lactate detection kits purchased from Nanjing Jiancheng Bioengineering Institute (cat. no. A09-2 and A154-1-1) were used to determine the glucose and lactate concentrations before and after 24 h of CC cell culture, following the manufacturer's protocols.

Co-immunoprecipitation (Co-IP). Co-IP assays were performed to detect the interaction between RACK1 and IGF1R using protein A/G magnetic beads (Bimake). The MS751 and SiHa cells were collected, lysed, and centrifuged at 4˚C and 12,000 x g for 20 min to obtain the supernatant, which was then mixed with primary antibody (Table SIII) and incubated overnight at 4˚C. Protein A beads were added and incubated at room temperature for additional 4 h. The beads were washed thrice with phosphate buffered saline-Tween 20 (PBST) for 5 min each time; 30 μl loading buffer were then added and boiled for 5 min at 100˚C. The supernatant was used for western blot analysis.

Immunofluorescence. The cells were seeded on coverslips and incubated with antibodies specific for IGF1R and RACK1 (Table SIII) at room temperature for 2 h. The coverslips were then incubated with Alexa Fluor 594 goat anti-rabbit IgG and Alexa Fluor 488 goat anti-mouse IgG (Table SIII) at room temperature for 2 h and stained with 4,6-diamidino-2-phenylindole (DAPI, MilliporeSigma) for at room temperature for 10 min. Randomized fields were imaged using a confocal laser microscope (LSM 980, Zeiss AG).

HLEC tube formation assay. Serum-free conditioned medium was prepared by culturing the CC cells ($1x10^7$ cells per 10 cm dish) in 10 ml serum-free medium for 24 h. The media were collected and centrifuged at 1,000 x g at room temperature for 5 min to remove cell debris and stored at 4˚C to concentrate the conditioned medium. The HLECs were seeded into 24-well plates (pre-coated with 100 μl Matrigel) containing cell conditioned medium and incubated for at 37˚C 10-16 h. Tube formation was quantified by measuring the total length of tube structures or the number of branch sites/nodes in three random fields under a microscope (Nikon E400, Nikon Corporation).

Dual luciferase reporter assay. A plasmid with the *RACK1* promoter was designed and constructed by Shanghai GeneChem Co., Ltd. The wild-type and mutant sequences of the *RACK1* promoter, GV712-*RACK1*-WT and GV712-*RACK1*-mut, respectively, were amplified and cloned into the GV712-basic vector. The cells were then collected and lysed at 48 h following transfected by using Lipofectamine® 3000 (Invitrogen; Thermo Fisher Scientific, Inc.), and the luciferase activity was detected using the dual luciferase reporter assay system (cat. no. E1910, Promega Corporation), and the reporter luciferase activity was normalized against *Renilla* luciferase activity.

Chromatin immunoprecipitation-PCR (ChIP-PCR). ChIP was performed according to the instructions provide with the SimpleChIP® enzymatic chromatin IP kit (agarose beads) (cat. no. 9002, Cell Signaling Technology, Inc.). The cells were ($1x10^7$) fixed with 1% formaldehyde for 10 min at room temperature, and fixation was terminated using 0.125 M glycine. The cell lysis buffer was then added, and the samples were sonicated to generate 200-1,000 bp fragments. The resulting cell lysates were immunoprecipitated using a POU2F2 antibody (ProteinTech Group, Inc.) and analyzed using RT-qPCR as described above. The cycling conditions were as follows: 94˚C for 60 sec; 57˚C for 30 sec; followed by 35 cycles at 72˚C for 30 sec, 72˚C for 2 min. Subsequently, 10 μl of each PCR product was removed for analysis using a 2% agarose gel. The anti-POU2F2 antibody and the primers used for the PCR of ChIP samples are listed in Tables SII and SIII.

Tumor xenograft model. All animal experiments were approved by the Ethics Committee of the First Affiliated Hospital of Xinjiang Medical University (authorization no. IACUC-20180223-128). Xenograft models were established and the study protocol was carried out as previously described (17,18). Female BALB/c nude mice were purchased from Beijing Vital River Laboratory Animal Technology Co., Ltd. The animals were kept under standard laboratory conditions (temperature, 22±2˚C; relative humidity, 50±10%; 12-h light/dark cycle) with access to food and water *ad libitum*. The female nude mice were 3 weeks old with an average weight of 12.82 g. A total of 32 nude mice were randomly assigned to four groups, and 8 nude mice were used per group. For the xenograft LNM model, $5x10^5$ MS751 and SiHa cells were inoculated into the footpads of the mice. The mice were euthanized via cervical dislocation 4 weeks after the first injection of tumor cells. Footpad tumors and popliteal lymph nodes were removed and stained with hematoxylin and eosin (H&E). Briefly, the tumor tissues were fixed in 4% paraformaldehyde for 7 days at room temperature, embedded in paraffin, then cut into 4-μm-thick sections. The slides were stained using the hematoxylin and eosin (H&E) staining lit (Beijing Solarbio Science & Technology Co., Ltd.), following the manufacturer's instructions.

IGF1 and rapamycin (Rapa) and 2-deoxy-D-glucose (2-DG) treatments. The CC cell lines were treated with the IGF1 (catalog no. 100-11; PeproTech, Inc.) at 200 ng/ml for 0, 6, 12 and 24 h at 37˚C. The cells in six-well plates were treated with IGF1 (200 ng/ml) and the mTOR inhibitor, Rapa (cat. no. AY-22989; MedChemExpress) at 10 or 20 nM for 24 h at 37˚C. Cells were harvested and used for protein isolation. Cervical cancer cells were treated 10 mM 2-DG (cat. no. HY-13966; MedChemExpress) at 37˚C for 24 h. The cells were harvested and used for Transwell invasion and migration assays, and the supernatant were used for HLEC tube formation assay.

Statistical analysis. The results are presented as the mean ± standard error of the mean (SEM). IBM SPSS Statistics for Windows, version 23.0 (IBM Corp.) and GraphPad Prism software (5.0 version; GraphPad Software, Inc.) were used for the statistical analyses. A two-tailed unpaired Student's t-test and one-way analysis of variance (ANOVA) with Tukey's post hoc test were used for comparisons between two or multiple groups, respectively. The associations between RACK1 expression and the patient clinicopathological characteristics were evaluated using Pearson's χ^2 test. Correlations between measured variables were analyzed using Spearman's rank correlation analysis. A value of $P<0.05$ was considered to indicate a statistically significant difference.

Results

RACK1 is highly expressed in CC cell lines, and regulates CC cell migration, invasion and lymphangiogenesis. The present study first evaluated the effects of RACK1 expression in patients with CC using published data. The analysis of the GEO database (GEO submission: GSE6791) revealed that RACK1 expression was higher in patient-derived CC tissues than in normal cervical tissues (Fig. S1A). However, the analysis of the GSE9750 dataset revealed that RACK1 expression was downregulated in CC tissues compared to normal cervical tissues (Fig. S1A). Subsequently, the analysis of the GSE26511 dataset revealed that RACK1 expression was not significantly associated with LNM (P=0.0706; Fig. S1B). Although no statistically significant differences were observed between CC and normal cervical tissues, RACK1 expression was positively associated with LNM. The mRNA and protein expression of RACK1 was then examined in the normal human cervical cell line, H8, and in four CC cell lines (Fig. 1A and B). RACK1 expression in the MS751 and SiHa cells was higher than that in the normal cervical cells; in particular, the MS751 cells, a CC cell line with a high metastatic potential, exhibited the highest RACK1 expression. These results suggest that RACK1 is a potential biomarker for human CC with LMN.

In the present study, two CC cell lines, MS751 and SiHa, were used to examine the biological function of RACK1. Non-specific control shRNA (shNON) and RACK1-shRNAs (shRACK1-1 and shRACK1-2) were transfected into the MS751 and SiHa cells, and stably transfected cell lines were established following selection with puromycin. The results revealed that *RACK1* knockdown effectively downregulated *RACK1* mRNA and protein expression in the MS751 and SiHa cell lines (Fig. 1C and D). Transwell assays using the MS751 and SiHa cells revealed that compared to the control group transfected with shNON, the shRNA-mediated silencing of *RACK1* decreased the invasive and migratory ability of the MS751 and SiHa cells (Figs. 1E and S1C). Consistent with these results, RACK1 knockdown decreased the expression of N-cadherin and promoted that of E-cadherin, which are essential proteins contributing to the invasiveness of cancer cells (Fig. 2C). Subsequently, the effect of RACK1 on the tube formation of HLECs, which is crucial for LNM in cancer, was evaluated. The culture supernatants from MS751 cells in which *RACK1* was knocked down inhibited the migration of the HLECs (Fig. 1F) and suppressed lymphangiogenesis (Fig. 1G). On the whole, these results demonstrated that RACK1 functioned as a critical tumor promoter and d contributed to the aggressiveness of CC cells.

RACK1 regulates glycolysis in CC cells. Metabolic changes play crucial roles in regulating cellular aggressiveness (19). As RACK1 is a crucial regulator of cellular function, it was hypothesized that RACK1 knockdown may contribute to the metabolic reprogramming of CC cells. To define the metabolic alterations induced by RACK1, the present study first examined the differential metabolites produced after knocking down *RACK1* in MS751 and SiHa cells using ^{1}H-NMR analysis. Table SIV presents 19 species of differential metabolites in shRACK1/MS751 cells compared to those in shNON/MS751 cells, among which, the levels of 13 species increased and those of 6 species decreased. Table SV shows 24 species of differential metabolites in shRACK1/SiHa cells compared to those in shNON/SiHa cells, among which, the levels of 16 increased and those of eight decreased. Moreover, 17 species of common differential metabolites were identified in the shRACK1/MS751 and shRACK1/SiHa cells, of which 13 were upregulated and 4 were downregulated (Table SVI). Of note, a significant association was found between RACK1 knockdown and the levels of common differential metabolites of glycolysis/gluconeogenesis using MetaboAnalyst 5.0 (https://www.metaboanalyst.ca/) (Fig. 2A and Table SVII). Aerobic glycolysis facilitates tumor metastasis by elevating glucose uptake and lactate production (20,21). Hence, the present study used glucose uptake and lactate production as glycolysis indices in CC cells. The results revealed that *RACK1* knockdown in the MS751 and SiHa cells significantly decreased glucose uptake by 63 and 56%, and lactate production by 66 and 63%, respectively, indicating that *RACK1* knockdown significantly suppressed glucose consumption and lactate production (Fig. 2B). Consistent with these observations, the glycolytic enzymes, hexokinase 2 (HK2), lactate dehydrogenase A (LDHA), glucose transporter 1 (GLUT1) and pyruvate kinase M2 (PKM2) were found to be downregulated by RACK1 knockdown (Fig. 2C and D). These results indicate that RACK1 enhances glycolysis by affecting the expression of relevant metabolic enzymes.

RACK1 affects glycolysis and lymphangiogenesis by interacting with IGF1R in CC cells. The present study then searched for candidate factors that interacted with RACK1 using Hitpredict and 263 candidates were identified. These factors were further mapped using Genemania, and four overlapping factors that interacted with RACK1 were considered

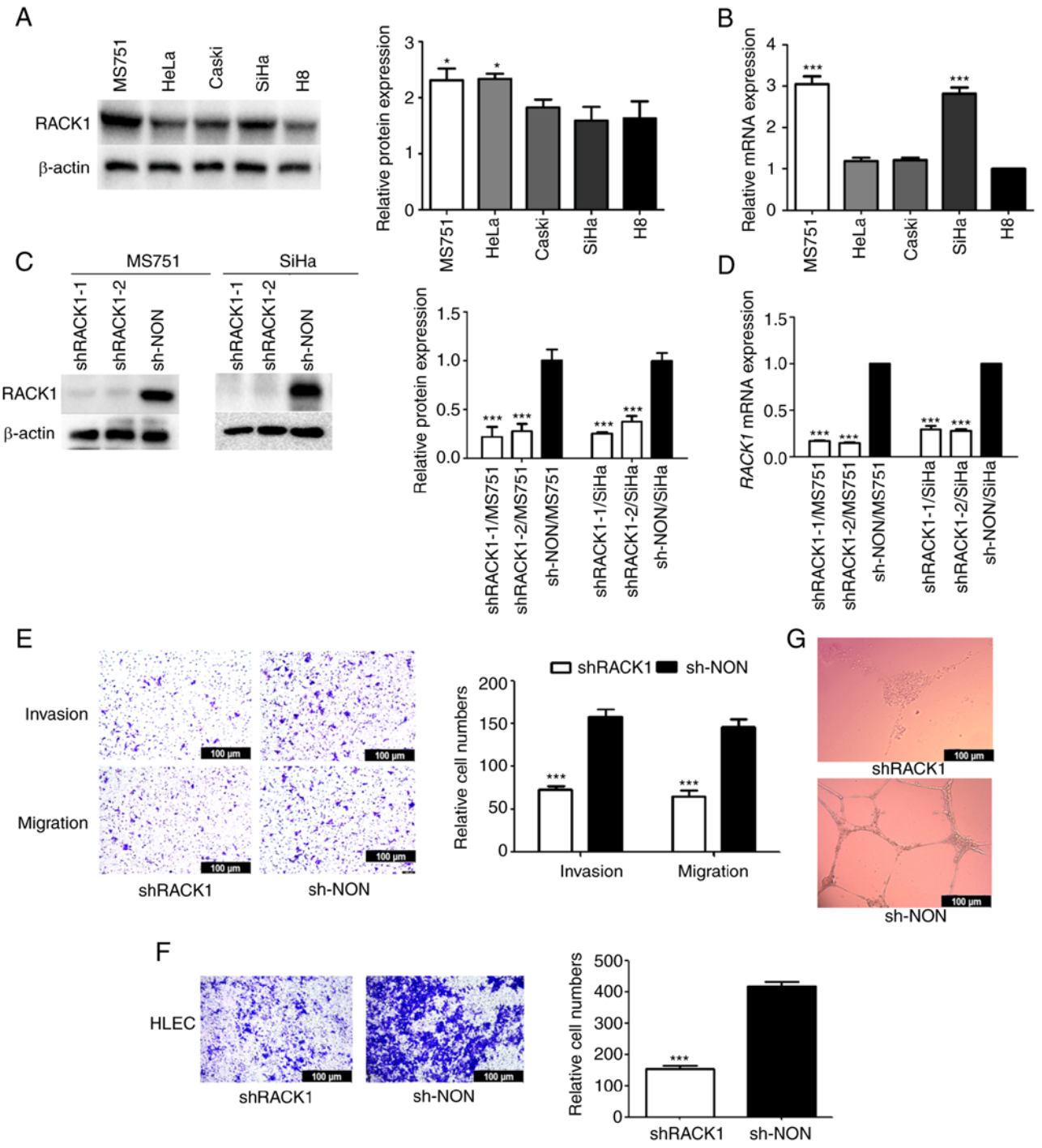

Figure 1. RACK1 is highly expressed in CC cell lines and regulates CC cell migration and invasion *in vitro*. (A) Protein levels of RACK1 in CC cell lines (MS751, HeLa, Caski and SiHa) and normal cell line (H8) detected using western blot analysis (left panel), with the protein bands assessed (right panel). (B) *RACK1* mRNA level in cell lines (MS751, HeLa, Caski, SiHa and H8) detected using RT-qPCR. (C) RACK1 expression in MS751 and SiHa cells transfected with specific shRACK1 lentiviral vectors (shRACK1-1 and shRACK1-2) was examined using western blot analysis and (D) RT-qPCR. (E) Transwell assays were performed to investigate the effects of RACK1 on the invasion and migration of MS751 cells (left panel), with the quantified bands assessed (right panel). (F) Transwell assays were performed to investigate the effects of RACK1 on the migration ability of HLECs (left panel), with the quantified bands assessed (right panel). (G) Effects of RACK1 on tube formation by HLECs. All data were obtained from three independent experiments. The data of two groups were analyzed using the Student's t-test and the data of more than two groups were analyzed using one-way ANOVA and are presented as the mean ± SD. Data were compared with the the H8 cell line or the shNON group (*P<0.05 and ***P<0.001). CC, cervical cancer; RACK1, receptor for activated C kinase 1; HLECs, human lymphatic endothelial cells; RT-qPCR, reverse transcription-quantitative PCR.

candidates (Fig. 3A). IGF1R has been reported to regulate the expression of glycolysis-related genes in various cancers (22). Previous studies have demonstrated that RACK1 interacts with IGF1R to influence its biological function in tumor cells (23,24). Subsequently, the present study investigated whether RACK1 interacts with the IGF1R in CC cell lines. The interaction between RACK1 and IGF1R was analyzed and demonstrated using a protein-protein molecular docking experiment. Co-IP analysis of CC cells demonstrated the exogenous interaction of RACK1 with IGF1R (Figs. 3C and S2A).

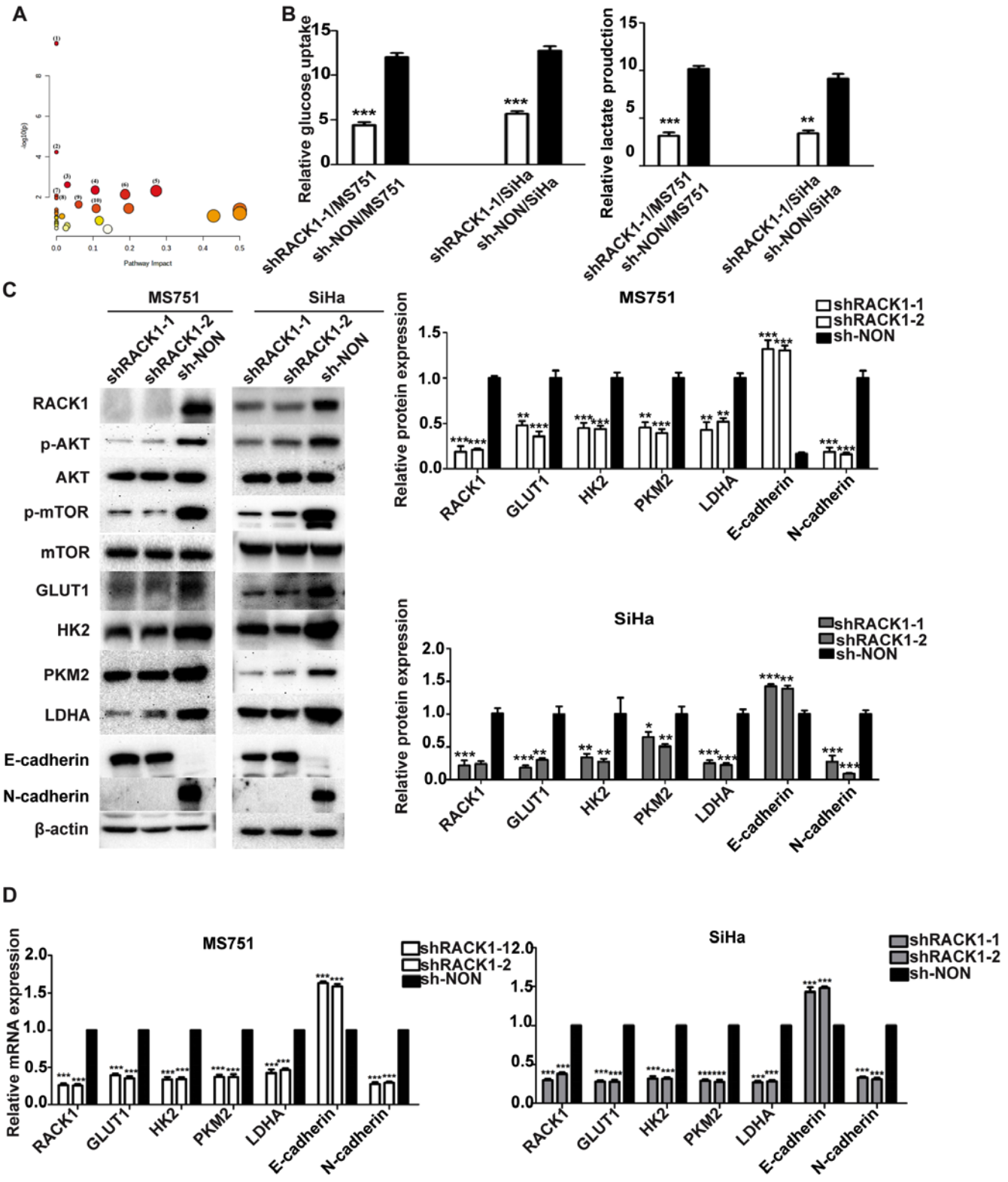

Figure 2. RACK1 enhances the glycolysis in cervical cancer cells. (A) Common differential metabolites in the metabolic pathway of the supernatant of shRACK1/MS751 and shRACK1/SiHa cells. (1) Aminoacyl-tRNA biosynthesis; (2) Valine, leucine and isoleucine biosynthesis; (3) glycolysis/gluconeogenesis; (4) Glyoxylate and dicarboxylate metabolism; (5) glycine, serine and threonine metabolism; (6) arginine and proline metabolism; (7) valine, leucine and isoleucine degradation; (8) butanoate metabolism; (9) pyruvate metabolism; (10) glutathione metabolism. (B) Effect of RACK1 on glucose uptake and lactate production. (C) Effect of RACK1 on the expression of the AKT/mTOR pathway, GLUT1, HK2, PKM2, LDHA, E-cadherin and N-cadherin, as evaluated using western blot analysis (left panel), with the protein bands assessed (right panel). (D) Effect of RACK1 on the mRNA expression of the GLUT1, HK2, PKM2, LDHA, E-cadherin and N-cadherin, as evaluated using reverse transcription-quantitative PCR analysis. All data were obtained from three independent experiments. The data of two groups were analyzed using the Student's t-test and the data of more than two groups were analyzed using one-way ANOVA and are presented as the mean ± SD. Data were compared with the shNON group (*P<0.05, **P<0.01 and ***P<0.001). RACK1, receptor for activated C kinase 1; mTOR, mammalian target of rapamycin; GLUT1, glucose transporter 1; HK2, hexokinase 2; LDHA, lactate dehydrogenase A; PKM2, pyruvate kinase M2.

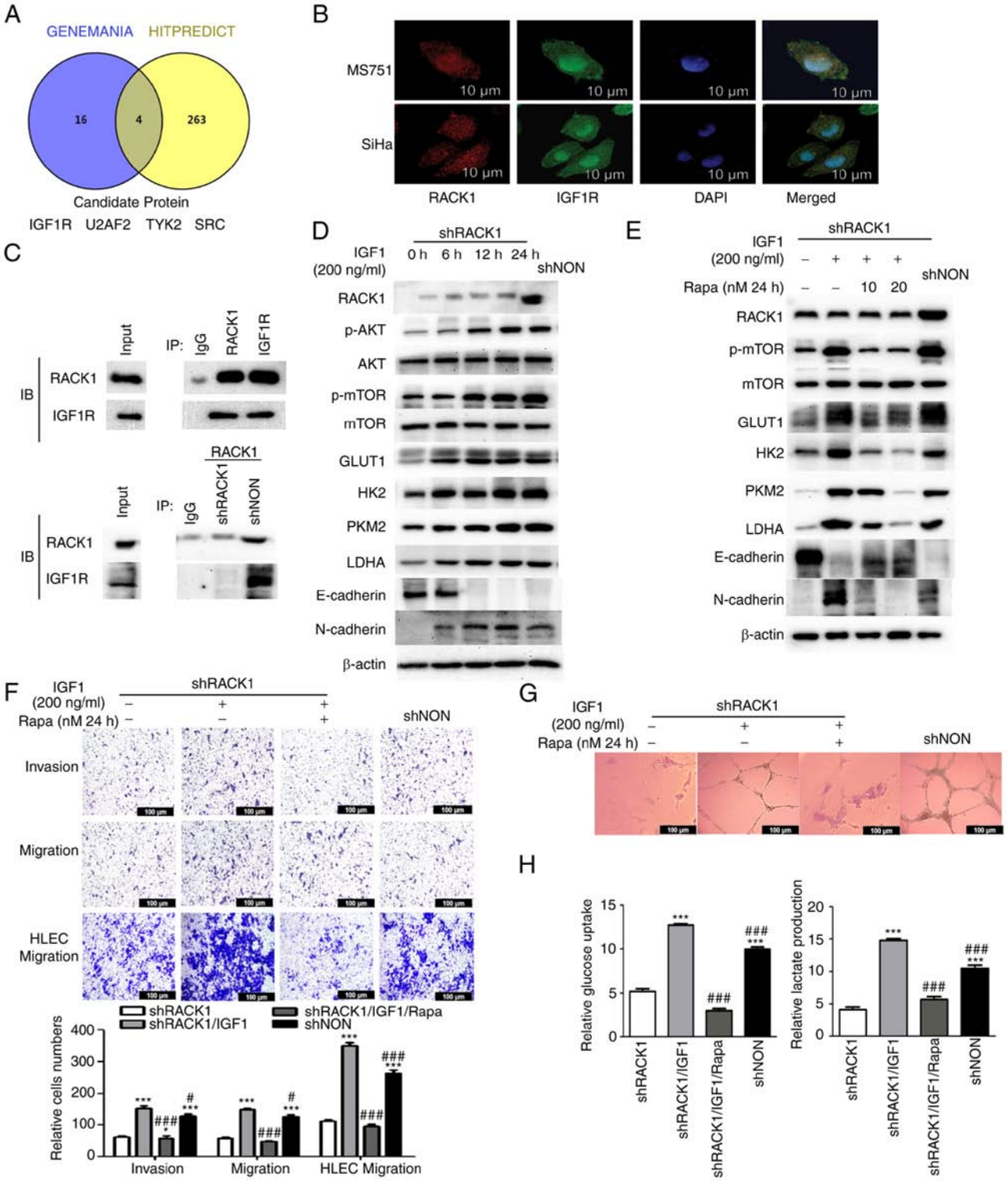

Figure 3. RACK1 interacts with IGF1R promotes the glycolysis, aggressiveness and lymphangiogenesis by activating IGF1R/AKT/mTOR signaling in MS751 cells. (A) Venn diagram showing the factors interacting with RACK1, co-existing in the Hitpredict and Genemania databases. (B) Association between RACK1 and IGF1R expression was analyzed using immunofluorescence staining in MS751 and SiHa cells. Nuclei were stained with DAPI (blue). (C) Co-IP assays were used to detect the interaction between RACK1 and IGF1R in MS751 cells (upper panel). Co-IP assay was used to detect the interaction between RACK1 and IGF1R in shRACK1/MS751 and shNON/MS751 cells (lower panel). (D) shRACK1/MS751 cells were stimulated for different time periods (6, 12 and 24 h) with 200 ng/ml IGF1. The RACK1, p-AKT (ser472 + ser474 + ser473), p-mTOR (ser2448), AKT, mTOR, GLUT1, HK2, PKM2 and LDHA, E-cadherin and N-cadherin expression was examined using western blot analysis. (E) shRACK1/MS751 cells were stimulated for 24 h with 200 ng/ml IGF1 and various concentrations (10 and 20 nM) of Rapa. The expression of RACK1, p-mTOR (ser2448), mTOR, GLUT1, HK2, PKM2, LDHA, E-cadherin and N-cadherin was examined using western blot analysis. (F) Transwell assays were performed to investigate the effects of IGF1 and IGF1 combined with Rapa on the invasion and migration of MS751 and HLECs cells (upper panel), with the quantified bands assessed (lower panel). (G) Effect of IGF1 and IGF1 combined with Rapa on tube formation by HLECs. (H) Effect of IGF1 and IGF1 combined with Rapa on glucose uptake and lactate production in MS751 cells. Data were analyzed using one-way ANOVA and are presented as the mean ± SD. Data were compared with the shRACK1 group (*P<0.05 and ***P<0.001). or shRACK1 + IGF1 group ($^{\#}$P<0.05 and $^{\#\#\#}$P<0.001). RACK1, receptor for activated C kinase 1; mTOR, mammalian target of rapamycin; GLUT1, glucose transporter 1; HK2, hexokinase 2; LDHA, lactate dehydrogenase A; PKM2, pyruvate kinase M2; Rapa, rapamycin; IGF1, insulin-like growth factor 1; HLECs, human lymphatic endothelial cells.

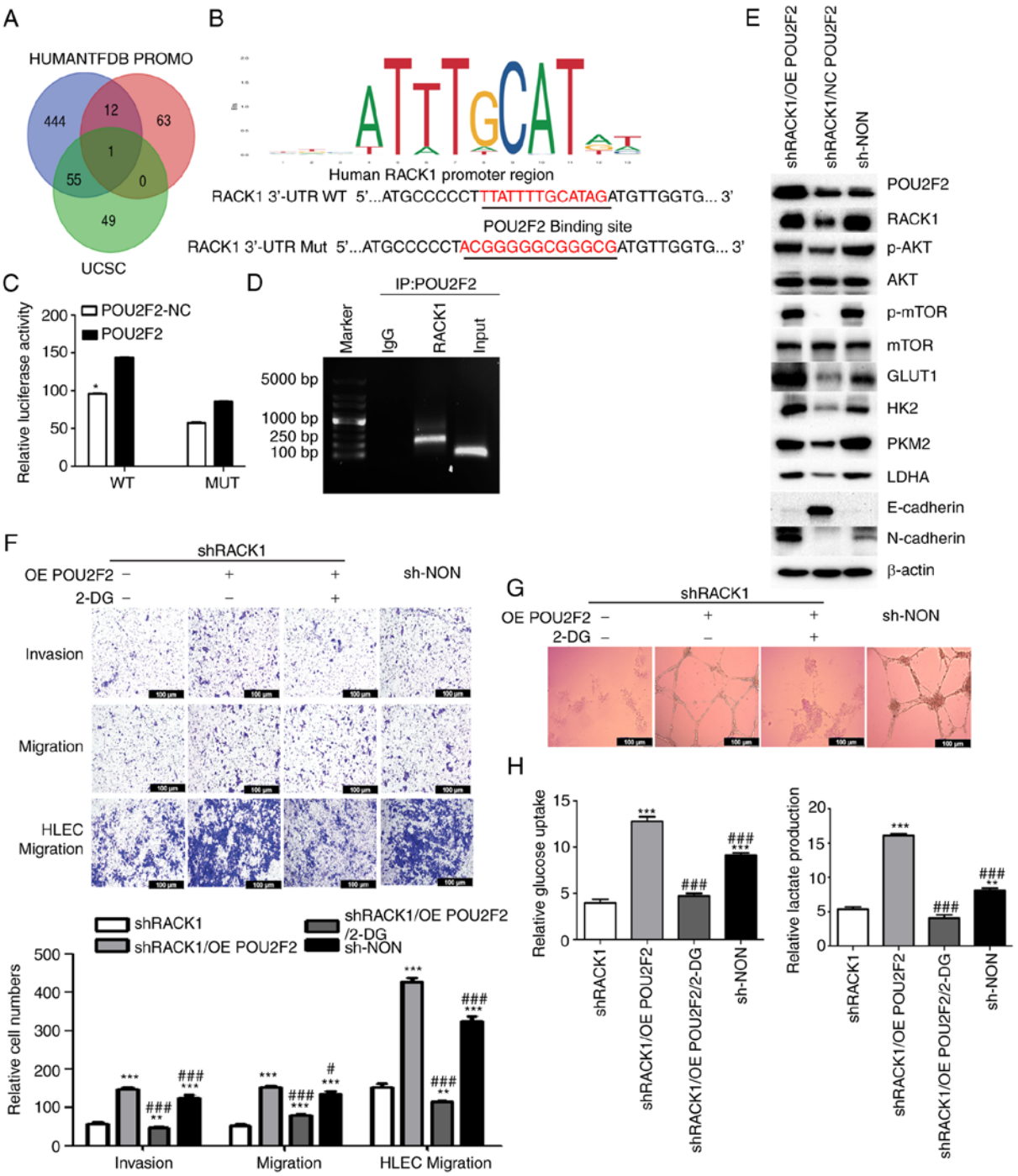

Figure 4. RACK1 is a direct target of POU2F2. (A) Venn diagram showing the transcription factor binding to RACK1 co-existing in UCSC, HUMANTFDB and PROMO database. (B) POU2F2 DNA binding sites are present in the human *RACK1* promoter region. The top panel shows the WT and MUT forms of the putative POU2F2 target sequences in *RACK1* 3'-UTR. Red font (upper panel) refers to the putative POU2F2 targeting sequence in the *RACK1* 3'-UTR. Red font (lower panel) refers to mutations in the POU2F2 targeting sequence in *RACK1* 3'-UTR. (C) Luciferase reporter assays of WT and MUT *RACK1* luciferase reporters transfected with POU2F2 in MS751 cells. (D) ChIP-PCR assay was used to detect POU2F2-binding sites in the sequence of the *RACK1* promoter. (E) Effect of POU2F2 on the expression of RACK1, p-AKT (ser472 + ser474 + ser473), p-mTOR (ser2448), AKT, mTOR, GLUT1, HK2, PKM2, LDHA, E-cadherin and N-cadherin in shRACK1/MS751 cells, as evaluated using western blot analysis. (F) POU2F2 OE-shRACK1/MS751 cells were stimulated for 24 h with 10 mM 2-DG. Effect of POU2F2 and 2-DG combined with POU2F2 on the invasion and migration of shRACK1/MS751 cells and migration of HLECs (upper panel), with the quantified bands assessed (lower panel). (G) Effect of POU2F2 on tube formation of HLECs. (H) Effect of POU2F2 on glucose uptake and lactate production in MS751 cells. Data were analyzed using one-way ANOVA and are presented as the mean ± SD. Data were compared with the shRACK1 group (**P<0.01 and ***P<0.001) or OE POU2F2/shRACK1 group ($^{\#}$P<0.05 and $^{\#\#\#}$P<0.001). RACK1, receptor for activated C kinase 1; POU2F2, POU class 2 homeobox 2; WT, wild-type; MUT, mutant type; 2-DG, 2-deoxy-D-glucose; mTOR, mammalian target of rapamycin; HK2, hexokinase 2; LDHA, lactate dehydrogenase A; GLUT1, glucose transporter 1; PKM2, pyruvate kinase M2; HLECs, human lymphatic endothelial cells; OE, overexpression.

Immunofluorescence revealed the colocalization of RACK1 and IGF1R in the cytoplasm of CC cells, which was consistent with the results of the Co-IP assay (Fig. 3B).

Previous research has demonstrated that the AKT/mTOR signaling pathway is a IGF1R target in cancer cells (25). Therefore, it was hypothesized that RACK1 may activate

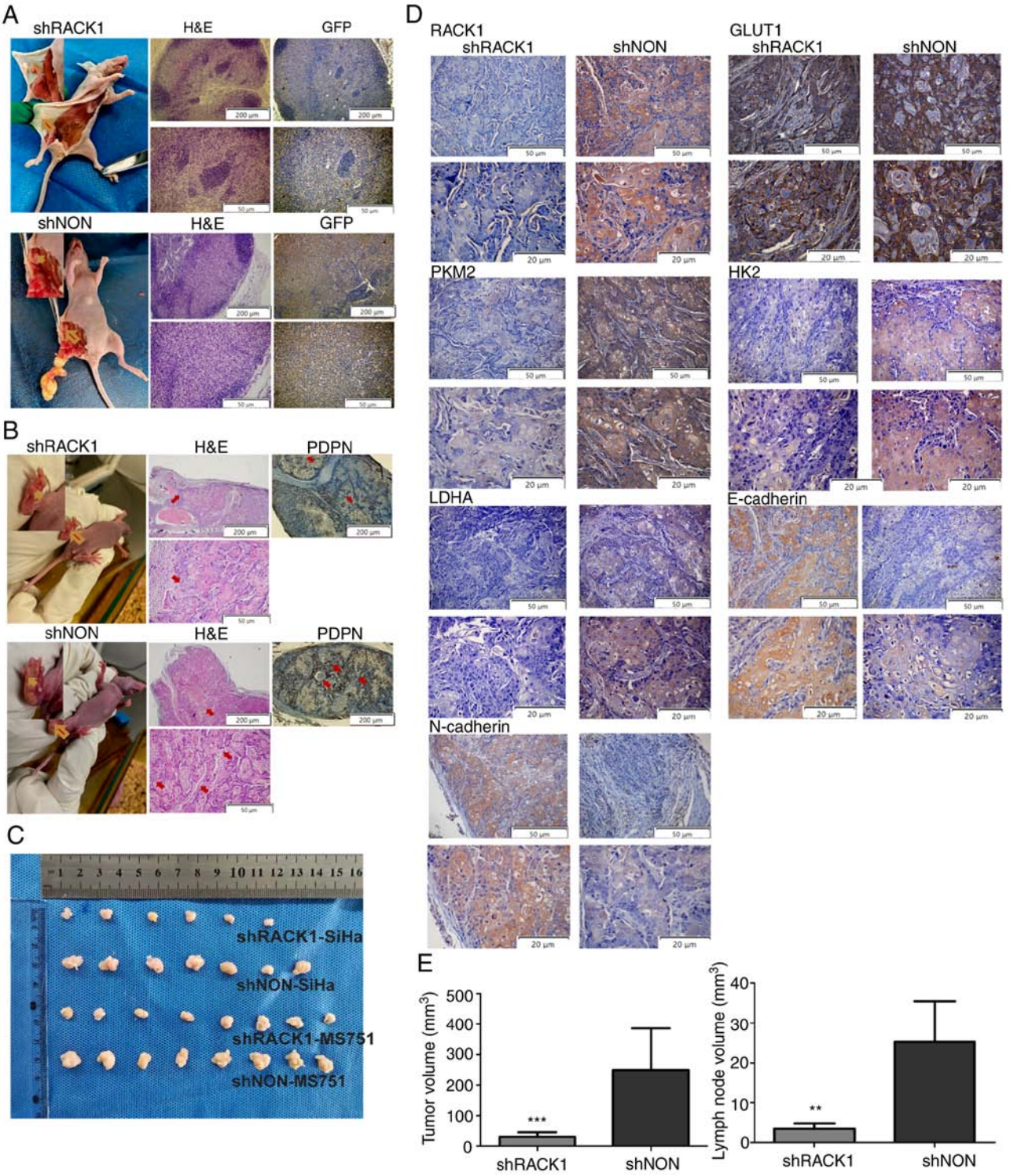

Figure 5. RACK1 enhances the LNM of MS751 cells *in vivo*. (A) Representative images of inguinal lymph nodes in different groups of nude mice (n=8, left panel). Representative images of inguinal lymph nodes of H&E staining in different groups of nude mice (middle panel). Representative images of anti-GFP IHC analysis for inguinal lymph nodes in different groups of nude mice (right panel). (B) Representative images of footpads primary tumor in different groups of nude mice (left panel). Representative images of footpads primary tumor tissues of H&E staining (middle panel) and percentages of PDPN-indicated lymphatic vessels density in different groups of nude mice (right panel). (C) The image of all tumors with a ruler. (D) Representative images of RACK1, GLUT1, PKM2, HK2, LDHA, E-cadherin and N-cadherin expression in footpad primary tumor tissues in IHC analysis. (E) The bar graph summarizes the tumor size assessed (left panel), and lymph node volume assessed (right panel). Data were compared with the shNON group (**P<0.01 and ***P<0.001). Data are presented as the mean ± SD and were analyzed using the t-test. IHC, immunohistochemistry; RACK1, receptor for activated C kinase 1; LNM, lymph node metastasis; HK2, hexokinase 2; LDHA, lactate dehydrogenase A; GLUT1, glucose transporter 1; PKM2, pyruvate kinase M2; PDPN, podoplanin.

AKT/mTOR signaling by interacting with IGF1R in CC cells. The expression patterns of the key genes involved in AKT/mTOR signaling, namely, phospho-AKT (ser472 + S474 + S473) (p-AKT), total AKT (AKT), and phospho-mTOR (S2448) (p-mTOR), were further validated by analyzing their post-transcriptional levels using western blot analysis

Table I. RACK1 expression in cervical carcinoma according to the histopathological characteristics of the patients with cervical cancer.

Characteristics	N	Negative	Weak	Moderate	Strong	χ^2	P-value
Cervical cancer tissues	104	21	24	43	16		
Cervicitis tissues	31	24	6	0	1	39.223	<0.001
Differentiation							
Well	20	1	1	10	8		
Moderate/poor	84	20	23	33	8	16.538	0.010
L/N metastasis							
Negative	57	17	15	17	8		
Positive	47	4	9	26	8	10.568	0.014
FIGO stage							
≤IIB	68	13	19	28	8		
>IIB	36	8	5	15	8	3.801	0.284
Tumor size							
<2.5 cm	51	14	8	22	7		
≥2.5 cm	53	7	16	21	9	5.237	0.155

RACK1, receptor for activated C kinase 1.

(Figs. 2C and S5A). It was observed that RACK1 knockdown significantly decreased the binding between RACK1 and IGF1R (Figs. 3C and S2A), and reduced the phosphorylation levels of AKT and mTOR, although the total AKT and mTOR expression levels were not markedly altered. Thus, it was hypothesized that RACK1 may positively regulate AKT/mTOR signaling by interacting with the IGF1R.

The present study then investigated the functional significance of IGF1R as regards the metabolic and metastatic roles of RACK1 in CC cells. It was found that IGF1 promoted AKT/mTOR signaling in CC cells. Moreover, IGF1 regulated the activation of AKT/mTOR signaling in CC cells in a time-dependent manner. The results of western blot analysis indicated that IGF1 significantly increased AKT and mTOR phosphorylation at 6, 12 and 24 h, and the level of AKT and mTOR phosphorylation was the highest at 24 h (Figs. 3D and S5B). Therefore, the 24 h time point was selected as the time point for the administration of IGF1 in subsequent experiments. It was found that the activation of AKT/mTOR signaling by IGF1 partially reversed the biological effects of RACK1. As was expected, the reduction in the invasiveness and migration (Figs. 3F and S2E) of CC cells, as well as the inhibition of the migration of HLECs (Fig. 3F) and lymphangiogenesis (Fig. 3G) induced by *RACK1* knockdown were largely reversed by IGF1 treatment. Consistent with this finding, it was observed that IGF1 treatment promoted N-cadherin and decreased E-cadherin expression in CC cells in which *RACK1* was knocked down (Figs. 3D, S2B, S3A and S4A). Subsequently, the present study investigated whether the activation of AKT/mTOR signaling by IGF1 was involved in RACK1-mediated glycolytic metabolism. IGF1 treatment increased glucose uptake and lactate production (Figs. 3H and S2C). Western blot analyses also confirmed that the expression of glycolysis-related enzymes in cells in which *RACK1* was knocked down returned to levels comparable to those in control cells (Figs. 3D, S2B, S3A and S4A). Hence, these results suggested that RACK1 contributed to the IGF1R-mediated aerobic glycolysis and lymphangiogenesis of CC cells.

RACK1 influences glycolysis and lymphangiogenesis by activating IGF1R/AKT/mTOR signaling. Previous research has demonstrated that the IGF1R/AKT/mTOR signaling pathway is associated with aerobic glycolysis in cancer cells (26). The present study further determined whether IGF1R/AKT/mTOR is involved in regulating CC cell glycolysis. For this purpose, a rescue experiment was performed to analyze the association between IGF1R and the AKT/mTOR signaling pathway. Rapa, an mTOR inhibitor, efficiently attenuated the IGF1-induced promotion of glycolysis in CC cells, as indicated by the level of glucose uptake and lactate production (Figs. 3H and S2C). Rapa also abrogated the increase in the IGF1-induced phosphorylation of mTOR and glycolysis-related enzyme expression (Figs. 3E, S2D, S3B, S4B and S5C). Furthermore, Rapa reversed the IGF1-induced promotion of the invasion and migration of CC cells and HLECs (Figs. 3F and S2E) and lymphangiogenesis (Fig. 3G). Subsequently, Rapa inhibition experiments were performed in IGF1-treated cells and it was observed that Rapa treatment considerably increased the expression of E-cadherin and decreased N-cadherin expression (Figs. 3E, S2D, S3B and S4B). Collectively, these results indicated that in CC cells, RACK1 promoted glycolysis, migration, invasion and lymphangiogenesis via IGF1R/AKT/mTOR signaling.

RACK1 is a direct target of POU2F2. Cancer metabolism is regulated by a complex network of different factors in various contexts (27). Hence, the present investigated the molecular

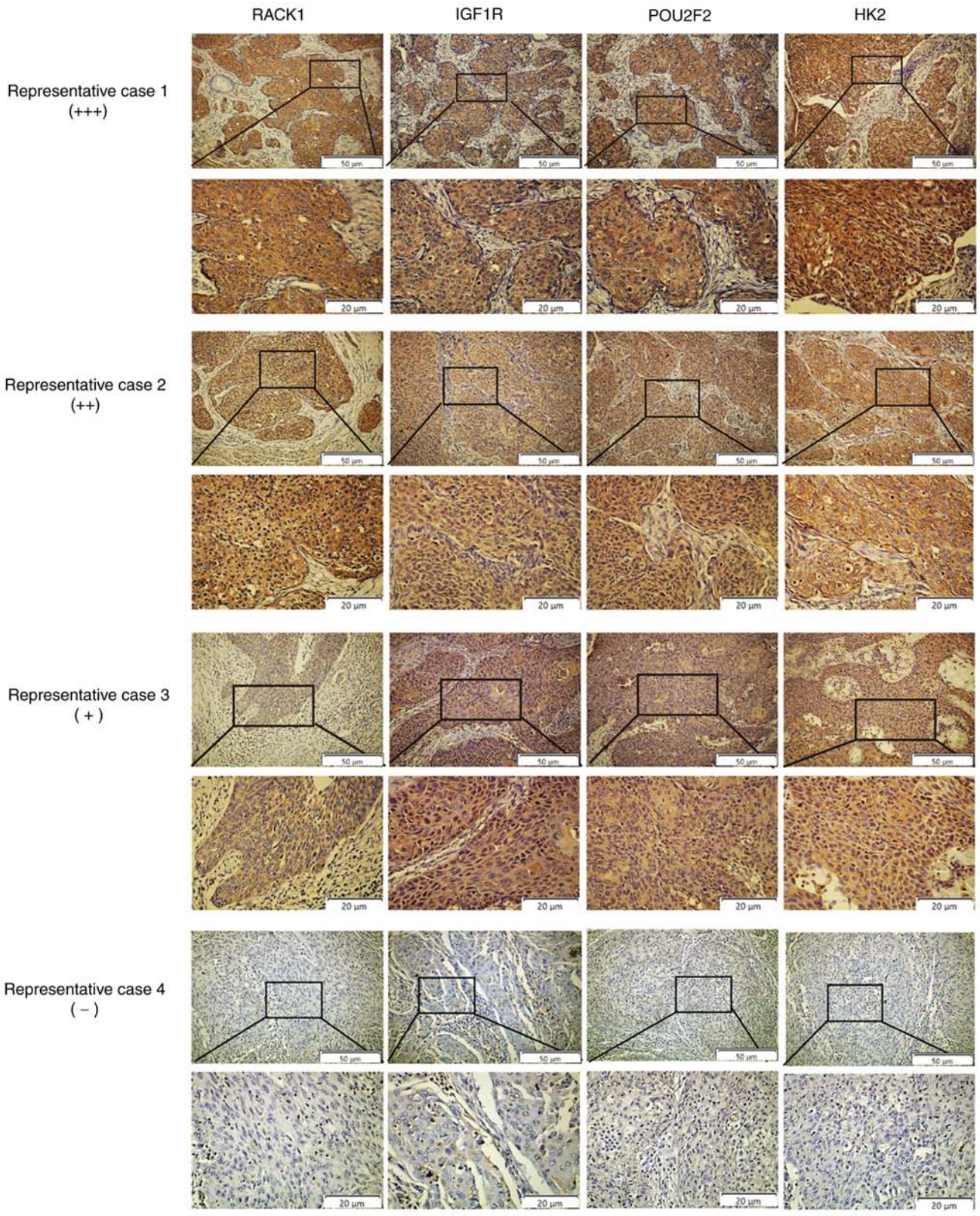

Figure 6. Associations between RACK1, IGF1R, POU2F2, and HK2 expression in tissues from patients with CC. Representative images of IHC staining in case 1 for RACK1, IGF1R, POU2F2 and HK2 (strong RACK1 expression). Representative images of IHC staining in case 2 for RACK1, IGF1R, POU2F2 and HK2 (medium RACK1 expression). Representative images of IHC staining in case 3 for RACK1, IGF1R, POU2F2 and HK2 (weak RACK1 expression). Representative images of IHC staining in case 4 for RACK1, IGF1R, POU2F2 and HK2 (negative RACK1 expression). CC, cervical cancer; IHC, immunohistochemistry; RACK1, receptor for activated C kinase 1; LNM, lymph node metastasis; HK2, hexokinase 2; LDHA, lactate dehydrogenase A; GLUT1, glucose transporter 1; PKM2, pyruvate kinase M2; IGF1R, insulin-like growth factor 1 receptor; POU2F2, POU class 2 homeobox 2.

mechanisms through which RACK1 mediates the activation of the IGF1R/AKT/mTOR signaling pathway and aerobic glycolysis. The upstream regulatory machinery of *RACK1* was also investigated. Three types of software (UCSC,

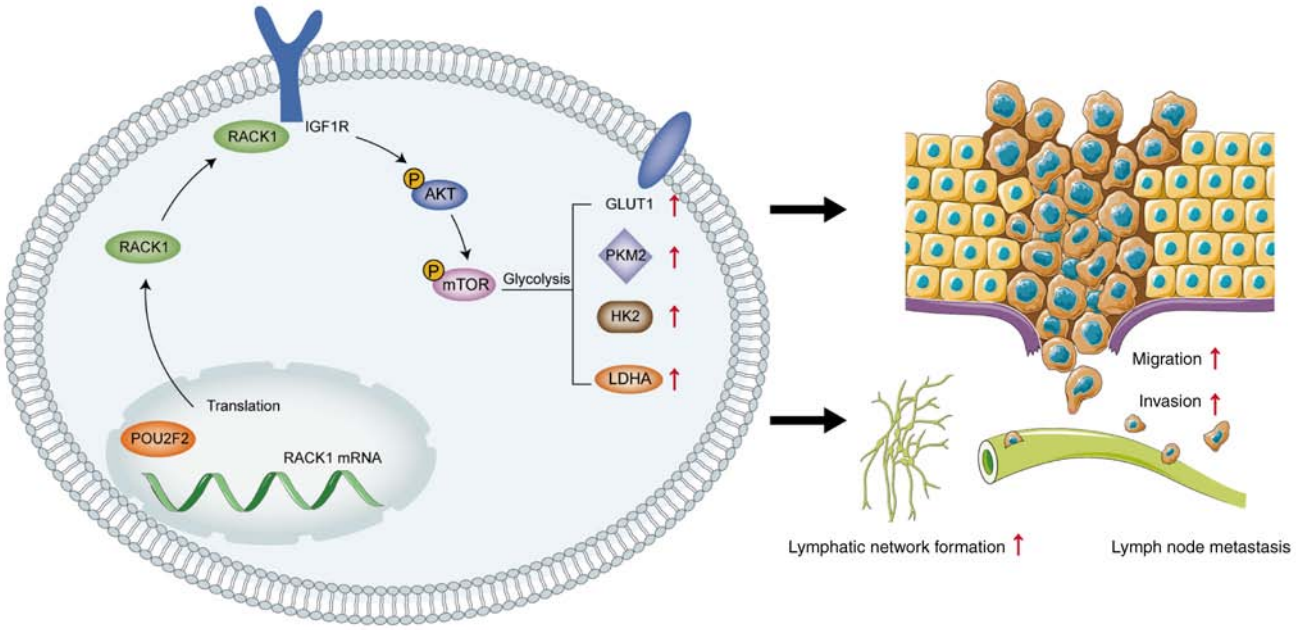

Figure 7. Schematic illustration of the mechanisms by which the POU2F2/RACK1/IGF1R/AKT/mTOR pathway promotes cell lymph node metastasis dependent on glycolysis. RACK1, receptor for activated C kinase 1; IGF1R, insulin-like growth factor 1 receptor; POU2F2, POU class 2 homeobox 2; mTOR, mammalian target of rapamycin; HK2, hexokinase 2; LDHA, lactate dehydrogenase A; GLUT1, glucose transporter 1; PKM2, pyruvate kinase M2.

HUMANTFDB and PROMO) were used to predict potential complementary base pairing between *RACK1* and transcription factors, and only POU2F2 was found to be present in the data from all three software packages (Fig. 4A). A previous study indicated that POU2F2 was expressed at significantly higher levels in CC (28). Recent research has also highlighted the importance of POU2F2 in glucose metabolism and its association with the oncogenic AKT/mTOR signaling pathway (29). Herein, the JASPAR database predicted a POU2F2 response element in the *RACK1* promoter (Fig. 4B). A dual-luciferase reporter assay was performed to confirm whether POU2F2 binds to the 3' untranslated region (3'UTR) of the *RACK1* mRNA. The relative luciferase activity was significantly high in the CC cells co-transfected with GV238-*RACK1*-3' UTR and the POU2F2 overexpression plasmid. The mutation of the 3'UTR of *RACK1* mRNA abrogated this effect (Figs. 4C and S6A), suggesting that POU2F2 binds to the 3' UTR of *RACK1* mRNA. Furthermore, the results of ChIP-PCR revealed that POU2F2 bound to the *RACK1* promoter in CC cells (Figs. 4D and S6B).

Subsequently, rescue experiments were performed by transfecting MS751 and SiHa cells with a POU2F2 overexpression plasmid to further investigate the effects of POU2F2 on RACK1/IGF1R/AKT/mTOR signaling pathway activation. Firstly, the overexpression of POU2F2 was validated using western blot analysis and RT-qPCR in two cervical cancer cells (Fig. S6C-E). Then we found that upon POU2F2 overexpression, *RACK1* expression levels increased to an extent similar to that observed in shNON cells (Figs. 4E, S3C, S4C and S6F). Moreover, POU2F2 overexpression abrogated the inhibitory effects of *RACK1* knockdown on migration and invasiveness of CC and HLECs (Figs. S6H and 4F), and lymphangiogenesis (Fig. 4G). The reduction in the phosphorylation levels of AKT and mTOR, and in the expression of glycolytic enzymes induced by *RACK1* knockdown was attenuated by POU2F2 overexpression (Figs. 4E, S3C, S4C, S5D and S6F). It was also observed that POU2F2 overexpression efficiently restored the levels of glucose uptake and lactate production inhibited by *RACK1* knockdown in CC cells (Figs. 4H and S6G). Based on these results, it was concluded that POU2F2 is required for RACK1-mediated aggressiveness and aerobic glycolysis by activating IGF1R/AKT/mTOR signaling.

RACK1 promotes CC invasion, migration and lymphangiogenesis by activating aerobic glycolysis. Increased aerobic glycolysis has been shown to be associated with various malignant phenotypes of cancer cells, including metastatic CC (30,31). In the present study, to determine whether the effects of RACK1 on CC cell aggressiveness are dependent on aerobic glycolysis, 2-DG, a glycolytic inhibitor, was added to the cell culture medium. 2-DG decreased the invasiveness and migration of CC and HLECs (Figs. 4F and S6H), as well as lymphangiogenesis (Fig. 4G), even following POU2F2 overexpression which resulted in RACK1 re-expression. In addition, the results revealed that POU2F2 overexpression increased N-cadherin and decreased E-cadherin expression (Figs. 4E, S3C, S4C and S6F). These results suggested that RACK1 may perform oncogenic functions in CC cells by activating CC cell aggressiveness in a glycolysis-dependent manner.

RACK1 promotes LNM and aerobic glycolysis of CC in vivo. To examine the effects of RACK1 on the growth and LNM of CC *in vivo*, shRACK1/SiHa, shNON/SiHa, shRACK1/MS751 and shNON/MS751 cells were injected into the footpads of mice to establish a xenograft model. After 4 weeks, the mice were euthanized, the size of the footpad tumors was measured and the inguinal lymph nodes were removed. Notably, the shRACK1/SiHa and shRACK1/MS751 injections prominently inhibited metastasis in the primary tumor of the inguinal lymph nodes of nude mice compared to those observed in

mice that received the shNON/SiHa and shNON/MS751 injections (Figs. 5A and S7A). As the lentiviral plasmids were labeled with green fluorescent protein (GFP), the transfected cancer cells that metastasized to the lymph nodes could be identified based on GFP fluorescence (Figs. 5A and S7A). The LNM rate was lower in the shRACK1/MS751 (25%, 2/8) and shRACK1/SiHa (37.5%, 3/8) groups than in the shNON/SiHa (87.5%, 7/8) and shNON/MS751 (87.5%, 7/8) groups. It was found that the tumor size and lymph node volume were smaller in shRACK1/MS751 and shRACK1/SiHa groups than in shNON/SiHa and shNON/MS751 groups (Figs. 5C and E, and S7D and E). Moreover, IHC revealed lower density of lymphatic vessels, as indicated by lower levels of podoplanin (PDPN) in the shRACK1/SiHa and shRACK1/MS751 groups than in the shNON/SiHa and shNON/MS751 groups (Figs. 5B and S7B), suggesting that RACK1 markedly induced LNM *in vivo*. Furthermore, the results revealed lower levels of N-cadherin, GLUT1, PKM2, HK2 and LDHA, and the higher expression of E-cadherin in the tissues from the shRACK1/SiHa and shRACK1/MS751 groups than in those of the shNON/SiHa and shNON/MS751 groups (Figs. 5D and S7C). Collectively, these findings revealed that downregulation of *RACK1* inhibited aerobic glycolysis and the aggressiveness of CC *in vivo*.

RACK1 expression correlates with POU2F2, IGF1R and HK2 expression in clinical CC specimens. To determine the association between RACK1 expression and aerobic glycolysis in clinical CC specimens, paraffin-embedded tissues from 104 clinical CC specimens were examined using IHC. The results revealed that RACK1 was more highly expressed in CC tissues than in normal cervical epithelial tissues. Moreover, RACK1 overexpression was significantly associated with tumor differentiation and positive lymph nodes, but not with tumor size or FIGO stage (Fig. S8A and Table I). Subsequently, the expression of RACK1, POU2F2, IGF1R and HK2 was profiled using IHC. Consistent with the observations in tumor cell lines and xenograft models, the distribution and intensity of RACK1 positively correlated with POU2F2, IGF1R and HK2 expression in CC tissues (Fig. S8B-D). As shown in Fig. 6, the CC samples exhibited a strong RACK1 expression, which was associated with a strong POU2F2, IGF1R, and HK2 expression (representative case 1). Similarly, CC samples with medium RACK1 levels expressed medium levels of POU2F2, IGF1R and HK2 (representative case 2). CC samples with a weak RACK1 expression expressed low levels of POU2F2, IGF1R and HK2 (representative case 3). CC samples not expressing RACK1 did not express POU2F2, IGF1R and HK2 (representative case 4). Taken together, these results suggest that the molecular mechanisms through which RACK1 induces aerobic glycolysis and LNM include the activation of the POU2F2-mediated IGF1R/AKT/mTOR signaling pathway in patients with CC (Fig. 7).

Discussion

LNM is associated with a poor prognosis of patients with CC, as effective treatment modalities are currently lacking (32). Therefore, the elucidation of the molecular mechanisms underlying LNM may provide clinically preventive and therapeutic strategies for patients with CC and LNM. However, the precise mechanisms underlying LNM in CC remain largely unknown. In the present study, the expression of RACK1 in CC and its key role in promoting LNM were investigated. It was observed that POU2F2 directly regulated RACK1, and that RACK1 interacted with IGF1R. Therefore, RACK1 links POU2F2 to the IGF1R/AKT/mTOR signaling pathway. The interaction of RACK1 with the POU2F2/IGF1R/AKT/mTOR pathway promoted CC glycolysis, and the subsequent regulatory effects on LNM was dependent on glycolysis (Fig. 7). These findings indicated that RACK1 plays a pivotal role in CC progression, indicating that RACK1 may be a potential therapeutic target for CC.

RACK1 has been described as one of seven critical network nodes with specific properties, which plays a critical role in the invasion and distant metastasis of tumors (33,34). Wu *et al* (14) observed the high and specific expression of RACK1 in metastatic CC tissue; however, Wang *et al* (35) observed a lower RACK1 expression in CC tissues than in normal cervical tissues. In the present study, the analysis of the data in the GEO database revealed that *RACK1* was upregulated or downregulated in CC. *RACK1* was upregulated in cancer tissues in the GSE6791 dataset, but was downregulated in cancer tissues in the GSE9750 dataset. Thus, the potential molecular mechanisms underlying the functions of *RACK1* in CC are unclear. In the present study, it was demonstrated that RACK1 was upregulated in CC tissues and cell lines, particularly in CC cells with a high metastatic potential (MS751 cell lines). Moreover, *RACK1* knockdown inhibited tumor cell invasion, migration and lymphangiogenesis, and reduced glycolysis *in vitro*. Furthermore, *RACK1* knockdown decreased the rate of LNM *in vivo*. The invasiveness of CC has been shown to be related to the acquisition of epithelial-to-mesenchymal transition (EMT) (36). It has also been observed that following the knockdown of *RACK1,* MS751 and SiHa cells exhibit an increased E-cadherin and decreased N-cadherin expression both *in vitro* and *in vivo*, which are critical markers of EMT (37), suggesting a novel mechanism by which RACK1 regulates invasion in CC. These data suggest that RACK1 may represent a potential molecular target for clinical intervention in patients with CC and LNM.

Alterations in the levels of intracellular metabolic intermediates that accompany cancer-associated metabolic reprogramming have profound effects on tumor progression (38). Accumulating evidence has demonstrated that glucose is required as an energy source, and that cellular glycolysis levels are crucial for cancer metastasis (11,39). Previously, the authors used ^{1}H NMR spectroscopy to analyze plasma samples from patients with cervical intraepithelial neoplasia (CIN) and CC, as well as normal individuals, and found aberrations in the levels of glycolysis-related enzymes (12). In addition, RACK1 is involved in glucose metabolism during cancer metastasis (40). PER1 utilizes the PER1/RACK1/PI3K/AKT pathway to promote glycolysis, and regulation of metastasis is dependent on glycolysis in oral squamous cell carcinoma (41). RACK1 interacts with FGFR to promote the phosphorylation of PKM2, thereby increasing tumor metastasis via glycolysis in lung squamous cell carcinoma (20). Hence, the present study investigated whether RACK1 modulates glycolysis to promote LNM in CC. The results of ^{1}H NMR analysis indicated

notable associations between RACK1 downregulation and the glycolysis/gluconeogenesis pathways. Consistent with the aforementioned findings, it was found that *RACK1* knockdown decreased intracellular glucose uptake and lactate production by downregulating the expression of key glycolytic enzymes in CC cells, such as GLUT1, PKM2, HK2 and LDHA. Therefore, the inhibition of aberrant glycolysis by targeting RACK1 may be a novel strategy for treating patients with CC with LNM. However, based on the results of ^{1}H NMR analysis, it was concluded that RACK1-induced metabolic changes involve not only aerobic glycolysis, but also glutamine metabolism; thus, this needs to be investigated in the future.

Another important finding of the present study is that RACK1 activated the AKT/mTOR pathway by interacting with IGF1R in CC. IGF1R plays a key role in regulating glucose metabolism and promotes cell invasion and metastasis (42). Previous studies have demonstrated the pro-tumor properties of IGF1R in CC (43,44). IGF1R is considered to be one of the regulators of the AKT/mTOR pathway. Kiely *et al* (45) identified RACK1 as an IGF1R-interacting protein that negatively affects the activation of the AKT pathway. However, Zhang *et al* (24) found that RACK1-IGF1R interaction resulted in the activation of AKT, but did not observe any change in AKT activation in MCF7 cells. In a recent study, RACK1 interacted with IGF1R, enabling activation of the AKT pathway, which favors the progression of prostate cancer (46) and renal cell carcinoma (47). The present study demonstrated that RACK1 interacted with IGF1R and that knockdown of *RACK1* decreased the binding of RACK1 with IGF1R, leading to inactivation of the AKT/mTOR pathway in CC cells. It has also been demonstrated that the aberrant activation of the AKT/mTOR pathway is associated with cancer progression (48,49). Moreover, the glycolytic processes regulated by the AKT/mTOR pathway is crucial for cancer metastasis (50), although the activation of the AKT/mTOR pathway by RACK1 in glycolytic processes and LNM in CC remains unknown. The present study performed rescue experiments to elucidate the mechanisms by which the AKT/mTOR pathway regulates CC cell lymphangiogenesis and glycolysis. The results revealed that IGF1 restored the activation of the AKT/mTOR pathway, and promoted cancer cell lymphangiogenesis and glycolysis in CC. Based on these results, it is suggested that RAPA, an mTOR inhibitor, inhibits CC cell progression and glycolysis by decreasing mTOR phosphorylation. These findings indicate that RACK1 constitutively activates the AKT/mTOR pathway, which is crucial for the progression and glycolysis of CC. However, IGF1R is not the only target of RACK1, as at least three factors have been predicted to interact with RACK1 using bioinformatics analysis. The precise molecular mechanisms through which RACK1 interacts with IGF1R in CC remain unclear. The identification of the minimal binding motif in RACK1 required for its interaction with IGF1R is thus warranted in the future.

A previous study reported the high expression of POU2F2 in tumor tissues and that it promotes tumorigenesis and metastasis (51). POU2F2 is a member of the POU transcription factor family that coordinates numerous cell responses, from internal cues of pluripotency and differentiation to external stimuli of proliferation and apoptosis, in a time- and cell-specific manner (52). Moreover, recent research has indicated that POU2F2 significantly promotes CC cell proliferation (28). However, the contribution of abnormal POU2F2 expression in LMN of CC remains unclear. In the present study, bioinformatics analysis revealed that POU2F2 was the only upstream regulator of RACK1 and was predicted to form complementary base pairs with RACK1. A POU2F2 binding sequence (5'-TTA TTTTGCATAG-3') was found in the *RACK1* promoter using JASPAR database prediction. It was found that POU2F2 overexpression restored the expression of RACK1 in shRACK1 cells. Herein, for the first time, to the best of our knowledge, it was demonstrated that POU2F2 transcriptionally activated RACK1 by directly binding to the *RACK1* promoter region from +680 to +692, thereby stimulating the AKT/mTOR signaling pathway, and promoting CC lymphangiogenesis and glycolysis. CC cells stably overexpressed POU2F2 when treated with 2-DG, a glycolysis inhibitor, in functional rescue experiments. It was found that the inhibition of glycolysis suppressed the migration and invasion observed with RACK1 re-expression upon the overexpression of POU2F2 in CC cells, indicating the critical role of aberrant glycolysis in RACK1-induced LNM in CC. Furthermore, the high expression of RACK1 was detected in the lymph nodes in clinical CC specimens, which positively correlated with POU2F2, IGF1R and HK2 expression in CC tissues. These results indicated that the POU2F2/RACK1/IGF1R/AKT/mTOR pathway may be a promising biomarker for CC. In addition, these findings improve the understanding of the upstream regulatory machinery of RACK1 and highlight a novel treatment strategy aimed at preventing RACK1-mediated CC LNM.

Acknowledgements

Not applicable.

Funding

The present study was funded by the Xinjiang Uygur Autonomous Region Science and Technology Plan Project, P.R. China (grant no. 2021D14002).

Availability of data and materials

The datasets used and/or analyzed during the current study are available from the corresponding author on reasonable request.

Authors' contributions

LX and AH designed the study. LX, JL, YH, MT, BM and HT performed the experiments. LX and JL drafted the manuscript. JL, HT and MT analyzed the data. AH managed the project administration. JL and BM confirm the authenticity of all the raw data. YH and BM processed the figures/images. All authors have read and approved the manuscript.

Ethics approval and consent to participate

The present study was performed in accordance with the guidelines of the Ethics Committee of the First Affiliated Hospital of Xinjiang Medical University. Written informed consent was

obtained from all patients and their relatives. The illiterate elderly patients authorized their children to sign the written informed consent these patients also placed a thumbprint on the written consent form to represent informed consent. All animal experiments were approved by the Ethics Committee of the First Affiliated Hospital of Xinjiang Medical University (authorization no. IACUC-20180223-128).

Patient consent for publication

Not applicable.

Competing interests

The authors declare that they have no competing interests.

References

1. Kagabu M, Yoshino N, Saito T, Miura Y, Takeshita R, Murakami K, Kawamura H, Baba T and Sugiyama T: The efficacy of a third-generation oncolytic herpes simplex viral therapy for an HPV-related uterine cervical cancer model. Int J Clin Oncol 26: 591-597, 2021.
2. Husaiyin S, Jiao Z, Yimamu K, Maisaidi R, Han L and Niyazi M: Thinprep cytology combined with hpv detection in the diagnosis of cervical lesions in 1622 patients. PLoS One 16: e0260915, 2021.
3. Yang H, Kuo YH, Smith ZI and Spangler J: Targeting cancer metastasis with antibody therapeutics. Wiley Interdiscip Rev Nanomed Nanobiotechnol 13: e1698, 2021.
4. Federico C, Sun J, Muz B, Alhallak K, Cosper PF, Muhammad N, Jeske A, Hinger A, Markovina S, Grigsby P, *et al*: Localized delivery of cisplatin to cervical cancer improves its therapeutic efficacy and minimizes its side effect profile. Int J Radiat Oncol Biol Phys 109: 1483-1494, 2021.
5. Swartz MA and Lund AW: Lymphatic and interstitial flow in the tumour microenvironment: Linking mechanobiology with immunity. Nat Rev Cancer 12: 210-219, 2012.
6. Fagiani E, Lorentz P, Bill R, Pavotbawan K, Kopfstein L and Christofori G: Vegf receptor-2-specific signaling mediated by vegf-e induces hemangioma-like lesions in normal and in malignant tissue. Angiogenesis 19: 339-358, 2016.
7. Liu D, Zeinolabediny Y, Caccuri F, Ferris G, Fang WH, Weston R, Krupinski J, Colombo L, Salmona M, Corpas R, *et al*: P17 from hiv induces brain endothelial cell angiogenesis through egfr-1-mediated cell signalling activation. Lab Invest 99: 180-190, 2019.
8. Park MK, Zhang L, Min KW, Cho JH, Yeh CC, Moon H, Hormaechea-Agulla D, Mun H, Ko S, Lee JW, *et al*: Neat1 is essential for metabolic changes that promote breast cancer growth and metastasis. Cell Metab 33: 2380-2397, 2021.
9. Vaupel P, Schmidberger H and Mayer A: The warburg effect: Essential part of metabolic reprogramming and central contributor to cancer progression. Int J Radiat Biol 95: 912-919, 2019.
10. Luo P, Zhang C, Liao F, Chen L, Liu Z, Long L, Jiang Z, Wang Y, Wang Z, Liu Z, *et al*: Transcriptional positive cofactor 4 promotes breast cancer proliferation and metastasis through c-myc mediated warburg effect. Cell Commun Signal 17: 36, 2019.
11. Yang J, Ren B, Yang G, Wang H, Chen G, You L, Zhang T and Zhao Y: The enhancement of glycolysis regulates pancreatic cancer metastasis. Cell Mol Life Sci 77: 305-321, 2020.
12. Hasim A, Ali M, Mamtimin B, Ma JQ, Li QZ and Abudula A: Metabonomic signature analysis of cervical carcinoma and precancerous lesions in women by (1)H NMR spectroscopy. Exp Ther Med 3: 945-951, 2012.
13. Wu J, Meng J, Du Y, Huang Y, Jin Y, Zhang J, Wang B, Zhang Y, Sun M and Tang J: Rack1 promotes the proliferation, migration and invasion capacity of mouse hepatocellular carcinoma cell line in vitro probably by pi3k/rac1 signaling pathway. Biomed Pharmacother 67: 313-319, 2013.
14. Wu H, Song S, Yan A, Guo X, Chang L, Xu L, Hu L, Kuang M, Liu B, He D, *et al*: Rack1 promotes the invasive activities and lymph node metastasis of cervical cancer via galectin-1. Cancer Lett 469: 287-300, 2020.
15. Tokunaga H, Shimada M, Ishikawa M and Yaegashi N: TNM classification of gynaecological malignant tumours, eighth edition: Changes between the seventh and eighth editions. Jpn J Clin Oncol 49: 311-320, 2019.
16. Livak KJ and Schmittgen TD: Analysis of relative gene expression data using real-time quantitative PCR and the 2(-Delta Delta C(T)) method. Methods 25: 402-408, 2001.
17. Liu D, Li C, Trojanowicz B, Li X, Shi D, Zhan C, Wang Z and Chen L: Cd97 promotion of gastric carcinoma lymphatic metastasis is exosome dependent. Gastric Cancer 19: 754-766, 2016.
18. Cui B, Chen J, Luo M, Liu YY, Chen HL, Lü D, Wang LW, Kang YZ, Feng Y, Huang LB and Zhang P: PKD3 promotes metastasis and growth of oral squamous cell carcinoma through positive feedback regulation with PD-L1 and activation of ERK-STAT1/3-EMT signalling. Int J Oral Sci 13: 8, 2021.
19. Bower AJ, Li J, Chaney EJ, Marjanovic M, Spillman DR Jr and Boppart SA: High-speed imaging of transient metabolic dynamics using two-photon fluorescence lifetime imaging microscopy. Optica 5: 1290-1296, 2018.
20. Li HM, Yang JG, Liu ZJ, Wang WM, Yu ZL, Ren JG, Chen G, Zhang W and Jia J: Blockage of glycolysis by targeting pfkfb3 suppresses tumor growth and metastasis in head and neck squamous cell carcinoma. J Exp Clin Cancer Res 36: 7, 2017.
21. Wan J, Liu Y, Long F, Tian J and Zhang C: Circpvt1 promotes osteosarcoma glycolysis and metastasis by sponging mir-423-5p to activate wnt5a/ror2 signaling. Cancer Sci 112: 1707-1722, 2021.
22. Lenz G, Hamilton A, Geng S, Hong T, Kalkum M, Momand J, Kane SE and Huss JM: T-darpp activates igf-1r signaling to regulate glucose metabolism in trastuzumab-resistant breast cancer cells. Clin Cancer Res 24: 1216-1226, 2018.
23. Hermanto U, Zong CS, Li WQ and Wang LH: RACK1, an insulin-like growth factor I (IGF-I) receptor-interacting protein, modulates IGF-I-dependent integrin signaling and promotes cell spreading and contact with extracellular matrix. Mol Cell Biol 22: 2345-2365, 2002.
24. Zhang W, Zong CS, Hermanto U, Lopez-Bergami P, Ronai Z and Wang LH: Rack1 recruits stat3 specifically to insulin and insulin-like growth factor 1 receptors for activation, which is important for regulating anchorage-independent growth. Mol Cell Biol 26: 413-424, 2006.
25. Lin T, Yang Y, Ye X, Yao J and Zhou H: Low expression of mir-99b promotes progression of clear cell renal cell carcinoma by up-regulating igf1r/akt/mtor signaling. Int J Clin Exp Pathol 13: 3083-3091, 2020.
26. Ellis BC, Graham LD and Molloy PL: Crnde, a long non-coding rna responsive to insulin/igf signaling, regulates genes involved in central metabolism. Biochim Biophys Acta 1843: 372-386, 2014.
27. Sun T, Liu Z and Yang Q: The role of ubiquitination and deubiquitination in cancer metabolism. Mol Cancer 19: 146, 2020.
28. Zhou L and Xu XL: Long non-coding rna arap1-as1 facilitates the progression of cervical cancer by regulating mir-149-3p and pou2f2. Pathobiology 88: 301-312, 2021.
29. Yang R, Wang M, Zhang G, Li Y, Wang L and Cui H: Pou2f2 regulates glycolytic reprogramming and glioblastoma progression via pdpk1-dependent activation of pi3k/akt/mtor pathway. Cell Death Dis 12: 433, 2021.
30. Guler OC, Torun N, Yildirim BA and Onal C: Pretreatment metabolic tumour volume and total lesion glycolysis are not independent prognosticators for locally advanced cervical cancer patients treated with chemoradiotherapy. Br J Radiol 91: 20170552, 2018.
31. Cegla P, Burchardt E, Roszak A, Czepczynski R, Kubiak A and Cholewinski W: Influence of biological parameters assessed in [18f]fdg pet/ct on overall survival in cervical cancer patients. Clin Nucl Med 44: 860-863, 2019.
32. Osaku D, Komatsu H, Okawa M, Iida Y, Sato S, Oishi T and Harada T: Re-classification of uterine cervical cancer cases treated with radical hysterectomy based on the 2018 figo staging system. Taiwan J Obstet Gynecol 60: 1054-1058, 2021.
33. Duan F, Wu H, Jia D, Wu W, Ren S, Wang L, Song S, Guo X, Liu F, Ruan Y and Gu J: O-glcnacylation of rack1 promotes hepatocellular carcinogenesis. J Hepatol 68: 1191-1202, 2018.
34. Han H, Wang D, Yang M and Wang S: High expression of rack1 is associated with poor prognosis in patients with pancreatic ductal adenocarcinoma. Oncol Lett 15: 2073-2078, 2018.
35. Wang J and Chen S: Rack1 promotes mir-302b/c/d-3p expression and inhibits ccno expression to induce cell apoptosis in cervical squamous cell carcinoma. Cancer Cell Int 20: 385, 2020.
36. Zhu X, Chen L, Liu L and Niu X: EMT-mediated acquired EGFR-TKI resistance in NSCLC: Mechanisms and strategies. Front Oncol 9: 1044, 2019.

37. Mahmood MQ, Ward C, Muller HK, Sohal SS and Walters EH: Epithelial mesenchymal transition (EMT) and non-small cell lung cancer (NSCLC): A mutual association with airway disease. Med Oncol 34: 45, 2017.
38. Torresano L, Nuevo-Tapioles C, Santacatterina F and Cuezva JM: Metabolic reprogramming and disease progression in cancer patients. Biochim Biophys Acta Mol Basis Dis 1866: 165721, 2020.
39. Li S, Zhu K, Liu L, Gu J, Niu H and Guo J: Lncarsr sponges mir-34a-5p to promote colorectal cancer invasion and metastasis via hexokinase-1-mediated glycolysis. Cancer Sci 111: 3938-3952, 2020.
40. Liang J, Yang Y, Bai L, Li F and Li E: Drp1 upregulation promotes pancreatic cancer growth and metastasis through increased aerobic glycolysis. J Gastroenterol Hepatol 35: 885-895, 2020.
41. Gong X, Tang H and Yang K: Per1 suppresses glycolysis and cell proliferation in oral squamous cell carcinoma via the per1/rack1/pi3k signaling complex. Cell Death Dis 12: 276, 2021.
42. Baserga R: The Igf-I receptor in cancer research. Exp Cell Res 253: 1-6, 1999.
43. Han L: Mir-99a inhibits proliferation and migration of cervical cancer cells by targeting igf1r. J BUON 26: 1782-1788, 2021.
44. Sin STK, Li Y, Liu M, Ma S and Guan XY: Trop-2 exhibits tumor suppressive functions in cervical cancer by dual inhibition of igf-1r and alk signaling. Gynecol Oncol 152: 185-193, 2019.
45. Kiely PA, Sant A and O'Connor R: Rack1 is an insulin-like growth factor 1 (igf-1) receptor-interacting protein that can regulate igf-1-mediated akt activation and protection from cell death. J Biol Chem 277: 22581-22589, 2002.
46. Caromile LA, Dortche K, Rahman MM, Grant CL, Stoddard C, Ferrer FA and Shapiro LH: Psma redirects cell survival signaling from the mapk to the pi3k-akt pathways to promote the progression of prostate cancer. Sci Signal 10: eaag3326, 2017.
47. He X, Wang J, Messing EM and Wu G: Regulation of receptor for activated c kinase 1 protein by the von hippel-lindau tumor suppressor in igf-i-induced renal carcinoma cell invasiveness. Oncogene 30: 535-547, 2011.
48. Wu Q, Ma J, Wei J, Meng W, Wang Y and Shi M: Foxd1-as1 regulates foxd1 translation and promotes gastric cancer progression and chemoresistance by activating the pi3k/akt/mtor pathway. Mol Oncol 15: 299-316, 2021.
49. Li ZQ, Qu M, Wan HX, Wang H, Deng Q and Zhang Y: Foxk1 promotes malignant progression of breast cancer by activating PI3K/AKT/MTOR signaling pathway. Eur Rev Med Pharmacol Sci 23: 9978-9987, 2019.
50. Zheng Y, Wu C, Yang J, Zhao Y, Jia H, Xue M, Xu D, Yang F, Fu D, Wang C, *et al*: Insulin-like growth factor 1-induced enolase 2 deacetylation by hdac3 promotes metastasis of pancreatic cancer. Signal Transduct Target Ther 5: 53, 2020.
51. Wang SM, Tie J, Wang WL, Hu SJ, Yin JP, Yi XF, Tian ZH, Zhang XY, Li MB, Li ZS, *et al*: Pou2f2-oriented network promotes human gastric cancer metastasis. Gut 65: 117-1438, 2016.
52. Bentrari F, Chantôme A, Knights A, Jeannin JF and Pance A: Oct-2 forms a complex with oct-1 on the inos promoter and represses transcription by interfering with recruitment of rna polii by oct-1. Nucleic Acids Res 43: 9757-9765, 2015.